11th International Workshop on Ship and Marine Hydrodynamics
Hamburg, Germany, September 22-25, 2019

Estimation of Flows around a Full-Scale Ship by Structured Overset RaNS Code "NAGISA"

Nobuaki SAKAMOTO[1,*], Hiroshi KOBAYASHI[1], and Kunihide OHASHI[1]

[1]National Maritime Research Institute (NMRI), CFD Research Group
6-38-1 Shinkawa Mitaka, 181-0004 Tokyo, Japan

*Corresponding author, sakamoto@nmri.go.jp

ABSTRACT

Viscous CFD simulations are carried out for conventional single-screw container ship "Sydney Express" in model and full scale using in-house finite volume RaNS solver NAGISA developed at NMRI. Structured grids are independently generated around hull and rudder, and domain connectivity information between the two blocks are calculated by in-house overset grid assembler UP_GRID also developed at NMRI. Rigorous validations are made both in model and full scale using available experimental data. In model scale, resistance and self propulsion coefficients are both well predicted by the present computation. Computational accuracy in nominal and total wake specifically at 12 o'clock and near the boss must be improved. In full scale, all the computational results and their validation against full scale measurement data indicate the importance of treatment of wall roughness. When the roughness is taken into consideration in full scale simulation, it contributes to improve computational accuracy in estimating propeller rotation speed and distribution of axial component of total wake in front of the propeller better than those of estimated without roughness.

1 INTRODUCTION

Different to the extensive studies in model scale[1][2][3], it may be less popular to utilize full scale viscous computational fluid dynamics (CFD) simulation in a design procedure of a ship. Several empirical assumptions and correlation factors, e.g. roughness allowance ΔC_F and wake ratio e_i, have been introduced to the conventional extrapolation methods to estimate delivered power in full scale from results in model scale. Recent developments in novel design of hull and energy saving devices (ESDs) sometimes make it difficult to utilize such correlation factors to estimate delivered power with conventional extrapolation methods. For instance, the well-known Yazaki's chart[4] to estimate e_i may no longer be valid when the ESDs are equipped on a ship and/or the main particular of a hull is out of the range of the chart. In the meantime, the design of ESDs is supposed to be based on the flow in full scale rather than in model scale as demonstrated by Inukai et al. (2011)[5] and Sakamoto et al. (2014, 2019)[6][7] since the flow in the stern vicinity drastically changes depending on Reynolds number (Rn). Viscous CFD simulations in full scale is able to reproduce the flow around hulls/ESDs at "in-service" configuration, therefore, it may contribute to come up with better methods in their performance evaluation and geometrical design once the computational methods are rigorously validated with full scale measurements. There are several research projects attempting to fill the "gap" between measurement and computation in full scale [8][9][10]. According to these backgrounds, the present study solves flows around a conventional container ship without ESDs in model and full scale by viscous CFD simulation. Rigorous validation studies in model scale are firstly carried out, and then total wake as well as several propulsion parameters are estimated by full scale simulation without/with surface roughness. These computational results are compared to the measurement data in full scale, and discussions are made in terms of the capability for present viscous CFD solver to estimate hydrodynamic performance and flows around a ship in full scale.

2 COMPUTATIONAL METHOD

The computational results are obtained in-house viscous CFD code NAGISA developed at National Maritime Research Institute (NMRI) in Japan[11]. It solves mass-conservation and Reynolds-averaged Navier Stokes equations by structured grid based finite volume method. The governing equations are non dimensionalized by length between perpendiculars (L_{pp}[m]), free stream velocity U_0[m/s], gravitational acceleration g[m/s^2] and kinematic viscosity ν[m^2/s]. The coordinate system is right-handed, x is positive from bow to stern, y is positive from port to starboard, and z is positive from keel to deck. The coordinate origin corresponds to the cross point of midship at ship centre line and still water line. As a turbulence model, explicit algebraic stress model based on k-omega base line formulation without rotational correction is selected. Wall roughness can be taken into consideration using the model proposed by Hellsten[12]. Free surface is modelled by single phase level-set method. Rotating propeller is modelled by simplified body force approach based on infinite bladed theory in which both axial and tangential components of velocity are considered for body force calculation. NAGISA can handle static and dynamic overset grid interface for which domain connectivity information (DCI) is computed by in-house overset grid assembler UP_GRID[13]. The solver is capable of handling ship motions in six degrees of freedom. Velocity and pressure are coupled by artificial compressibility approach. Matrix system is solved using symmetric Gauss-Seidel method which is efficiently parallelized by OpenMP® on shared memory machine. In the momentum equation, the 3rd order Monotone Upwind Scheme for Conservation Laws (MUSCL) scheme is utilized for special discretization in convection term and diffusion term is discretized by 2nd order central differencing scheme. The 1st order Euler backward scheme is utilized for temporal discretization, and steady state simulations are carried out with local time stepping.

3 TEST CASES

3.1 Geometry

Figure 1 shows overview of the target hull "Sydney Express". It was subjected to full scale measurements in terms of free air content, total wake, propeller cavitation pattern and pressure fluctuation in the stern vicinity[14][15]. The ship was also utilized as one of the benchmark cases for studies in cavitation organized by International Towing Tank Conference (ITTC) in 1980's to 1990's[16][17] as well as for the studies in European Union (EU) project in the middle to 2000's[4]. "Sydney Express" is a conventional single-screw container ship with rudder. No ESDs were equipped. Table 1 describes the major dimension of the hull and its propeller. In Table 1, B is the moulded breadth, d is the design draught, C_B is the block coefficient, D_p is the diameter of the propeller, P/D_p is the mean pitch ratio, A_e/A_o is the expanded area ratio and Z is the number of blades.

Figure 1: Overview of Sydney Express

Table 1: Major dimension of "Sydney Express" and its propeller

Hull		Propeller	
L_{pp}(m)	210.00	D_p(m)	7.00
B(m)	30.50	P/D_p	0.936
d(m)	11.00	A_e/A_o	0.78
C_B	0.616	Z	5

3.2 Flow Condition, Running Attitude and Wall Roughness

Table 2 summarizes flow condition, running attitude of the ship and treatment of wall roughness for each simulation presented in this manuscript. Two non-dimensional parameters (Froude number: Fn and Rn) are specified to identify flow conditions. When validating resistance and self propulsion coefficients in model scale, the ship is free to sink and trim during the simulation while it is fixed at given draught and trim for validation studies of local flow in model and full scale. In the present study, model scale validations in resistance and self propulsion coefficients as well as in nominal and total wake are carried out prior to full scale study to confirm fundamental accuracy of the CFD solver. Full scale computations are then carried out in double-model configuration. The effect of free surface in full scale simulation is taken into consideration as a part of propeller load, e.g. wave making resistance coefficient is computed in model scale, and then it is added to total resistance coefficient in self propulsion configuration in full scale. The roughness height k_s(μm) is set according to the review by Orito and Kakinuma (1980)[18].

Table 2: Flow condition, running attitude of the ship and wall roughness in the present CFD simulations in model(#1, #2) and full (#3) scale

#	**Flow condition (Fn, Rn)**	**Running attitude**	**Wall roughness**	**Purpose of computation**
1	(0.21, 9.04E+06) (0.23, 9.90E+06) (0.25, 1.08E+07)	Free to trim and sink from even-keel design draught	Smooth	Validation of resistance and self propulsion coefficients in model scale
2	(0.0, 1.51E+07) (0.229, 1.51E+07)	Fixed trim and sink during simulation. Static trim and sinkage given according to measured values.	Smooth	Validation of nominal and total wake in model scale
3	(0.0, 1.86E+09) Ship speed corresponds to Fn=0.231.		Smooth k_s=90(μm)	Validation of total wake and propulsion parameters in full scale

3.3 Grid and Boundary Conditions

Figure 2 shows the computational grid in the vicinity of bow and stern below still water line, respectively, and Table 3 summarizes the number of cells for each block. Structured grid is generated around hull and rudder independently utilizing commercial grid generation package Gridgen® ver15.18, and the mesh regions are overlapping. The DCI between the two blocks is calculated by UP_GRID[12] prior to the simulations. Two types of grid topologies, e.g. OO and HO, are prepared for hull block at first in order to determine the better topology for the hull block to capture the wake pattern accurately. Although the result is not shown herein, initial validation study for nominal wake in model scale concluded that both topologies give almost the same results. Consequently, OO topology is adopted for hull block. Minimum spacing next to the wall is set according to the criteria suggested by ITTC Recommended Procedures and guidelines[1] so that non-dimensional wall distance y+ becomes nearly 1 to 2 which is the requirement for the near wall turbulence model utilized in the present study.

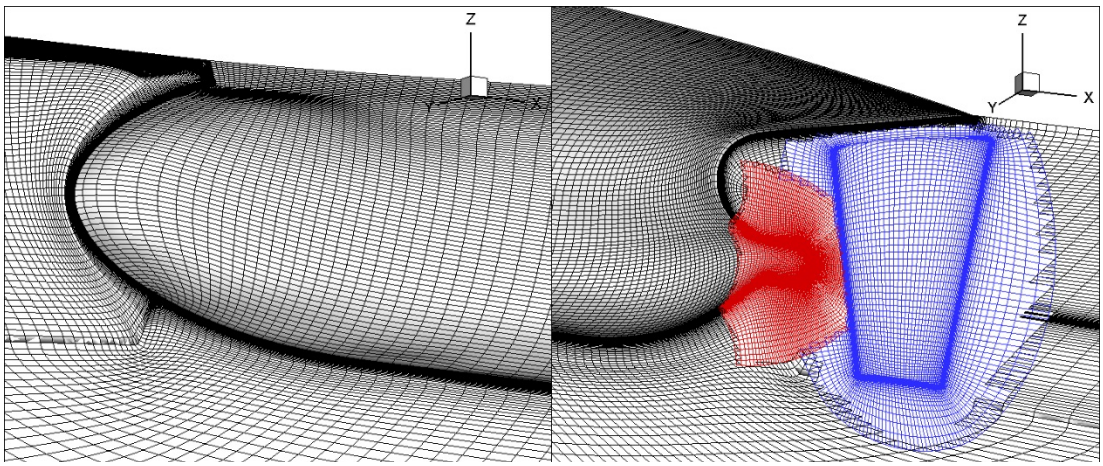

Figure 2: Computational grid (OO topology for the hull) in the stern vicinity: bow (left) and stern (right)

Table 3: Number of cells for each block

	(i, j, k)	total
Hull (OO topology)	(172, 192, 148)	4,887,552
Rudder	(60, 80, 52)	249,600
Stern tube	(60, 80, 108)	518,400
External	(20, 40, 12)	9,600
Grand total		5,665,152

In Table 3, i-j-k correspond to streamwise, girthwise and normal directions, respectively, for the hull and stern tube while they are chord-normal, chordwise and normal directions, respectively, for the rudder.

The size of external computational domain is $-5.0 \leq x/L_{pp} \leq 10.0, -5.0 \leq y/L_{pp} \leq 5.0, -5.0 \leq z/L_{pp} \leq 0.0(double\ model), 0.038(with\ free\ surface)$. The forward perpendicular (FP) and aft perpendicular (AP) correspond to $x/L_{pp} = -0.5$ and 0.5, respectively. The boundary conditions utilized in the present study are inflow, outflow, no-slip wall, and z-symmetry/far field.

3.4 Validation Data and Variables

In model scale, resistance, propeller open water characteristics (POC), self propulsion quantities, nominal and total wake are subjected to validation. Once the total resistance coefficient C_{tm} is defined, residuary resistance coefficient C_r is obtained based on two dimensional extrapolation method together with the frictional resistance coefficient C_{f0m} from Schoenherr's formula. The POC subjected to the validation are the thrust coefficient K_T, the torque coefficient K_Q and open water efficiency η_o as a function of advance coefficient J. Self propulsion analysis is made by K_T-identity method at ship-point to obtain thrust deduction coefficient 1-t, effective wake coefficient in model scale 1-w_{tm}, and relative rotative efficiency η_R. Experimental data from Ukon (1991)[17] are utilized to validate POC, resistance and self propulsion coefficients. For velocity field, experimental data provided by Hamburg Model Ship Basin (HSVA) are made use of to validate nominal wake measured at x/L_{pp}=0.478 and total wake measured at x/L_{pp}=0.472, 0.476 and 0.478.

In full scale, computational results of propeller rotation speed n_p(rps), torque Q(N-m), shaft power P_D(MW) and axial component of total velocity at x/L_{pp}=0.477 are validated using full scale measurement data. The flow condition (Fn, Rn) at full scale measurement is (Fn, Rn)=(0.231, 1.859E+09). Two additional criteria are adopted to investigate quantities of ship wake in full scale. To extrapolate axial component of ship wake from model to full scale, Sasajima-Tanaka's method[4] is utilized in which potential wake component is estimated by Hess-Smith panel method. Extrapolated nominal wake is compared to the wake directly estimated via full scale CFD simulation. The e_i $(= (1 - w_{ts})/(1 - w_{tm})$ where 1-w_{ts} is the effective wake coefficient in full scale) is estimated according to Yazaki's chart with 1-w_{tm} estimated by model scale CFD simulation. This parameter is also compared to the value for which 1-w_{ts} is directly estimated by full scale CFD simulation.

4 RESULTS AND DISCUSSION

4.1 Model Scale

Figure 3 shows experimental and computational results of POC as well as resistance and self propulsion coefficients in model scale. The body force model accurately estimates POC over entire range of J. According to the experimental data[16], the working point of this propeller around design speed of the ship lies in between J~0.6 to 0.7. In this region, the difference in POC between experiment and computation is approximately 1%in K_T, 0.05% in K_Q and 1.2% in η_o, respectively. It indicates that the possible source of difference in 1-w_{tm} between experiment and computation originated from POC is 1%. The computational results of C_{tm} agree quite well with the experiment within 2% of difference at $0.21 \leq Fn \leq 0.25$. For self propulsion coefficients, the difference between experiment and computation is approximately 0.5% in 1-t, 4% in 1-w_{tm} and 2% in η_R, respectively. The difference in 1-w_{tm} is larger than those of 1-t and η_R which is most probably due to computational accuracy in nominal wake distribution discussed later in this section. Figure 4 describes computational result of wave pattern around the hull at Fn=0.231 in model scale for which it is the same Fn as the full scale measurement. The result shows developed Kelvin wave pattern. Breaking bow wave is not captured by the present grid resolution at Fn=0.231.

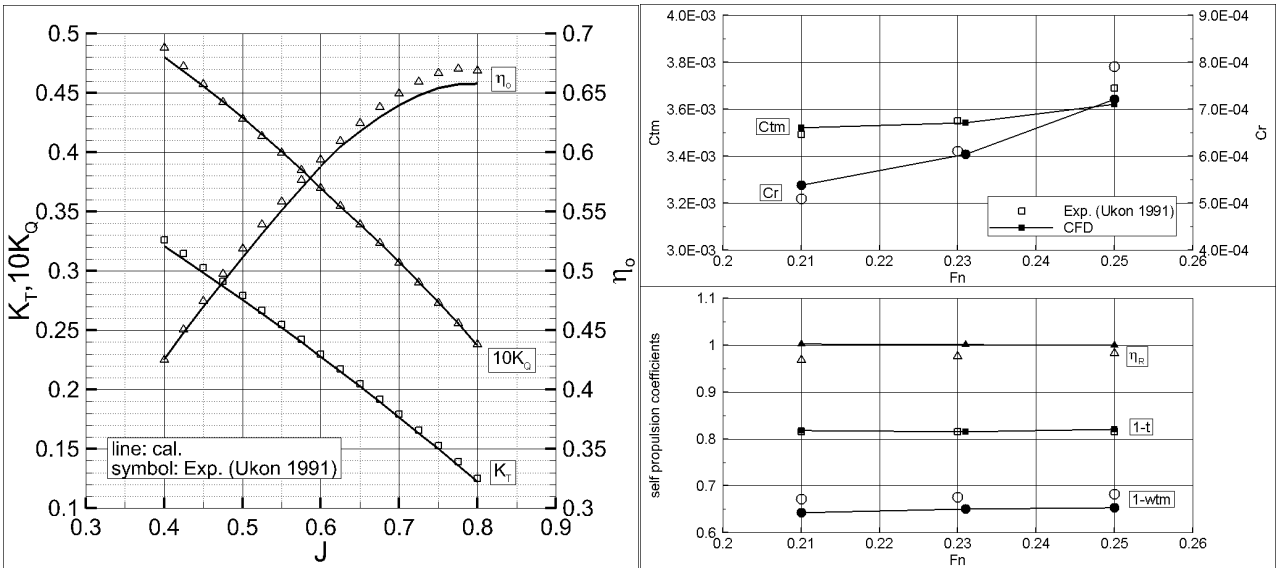

Figure 3: Experimental and computational results of POC (left) and resistance and self propulsion coefficients (right) in model scale

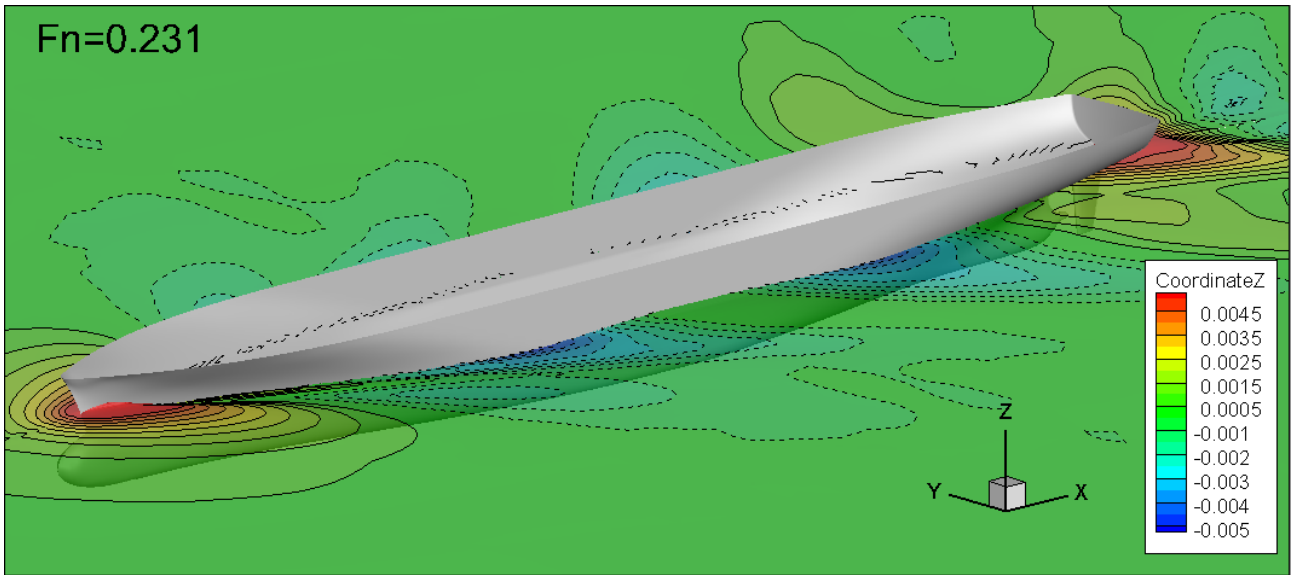

Figure 4: Computational result of wave pattern around the hull at Fn=0.231 in model scale

Figures 5 and 6 show experimental and computational results of nominal and total wake distribution, respectively, in the vicinity of propeller plane. For nominal wake distribution, the present computation captures the global trend of the wake pattern, yet shows some local discrepancies compared to the experiment. The computational result shows larger value (i.e. faster axial velocity) at 12 o'clock region, in the meantime, the region of low axial velocity in the vicinity of the bottom half of the boss is smaller than that of the experiment. Axial velocity at r/R=0.9 and 1.0 in computation is lower than that of the experiment. Similar computational trend can be observed in Schweighofer et al. (2005)[19], and these differences cause discrepancy in 1-w_{tm} reported in Fig. 3. Adoption of HO-topology in hull block increases the resolution close to the wall yet it does not contribute to improve these differences. Sakamoto et al. (2011)[20] reported that such discrepancy can be improved by adding excessive rotational correction in turbulence model yet it yields another discrepancy in resistance and self propulsion coefficients. In consequence, the reason of these differences is not likely due to spacial resolution, rather it could be due to modeling of eddy viscosity at near wall region. For total wake distribution, the present computation also captures the global trend. Asymmetric wake pattern caused by induced velocity from propeller rotation can be observed both in the experiment and computation at x/L_{pp}=0.476 and 0.478. The differences between the experiment and computation observed at nominal wake can still be seen in total wake but they become less apparent.

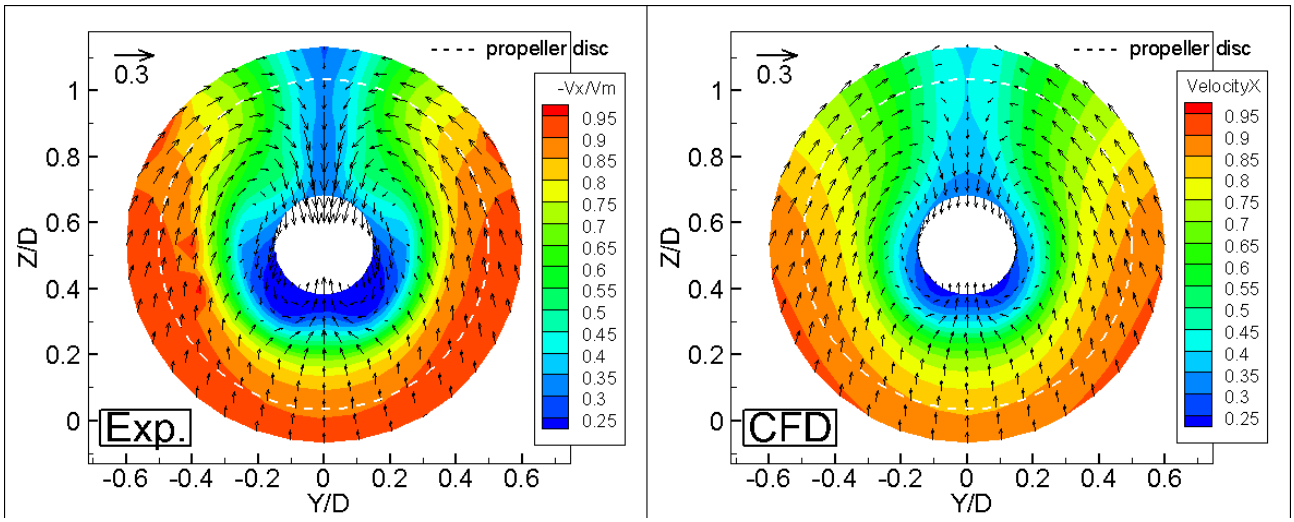

Figure 5: Experimental (left) and computational (right) results of nominal wake distribution in model scale at x/L_{pp}=0.478

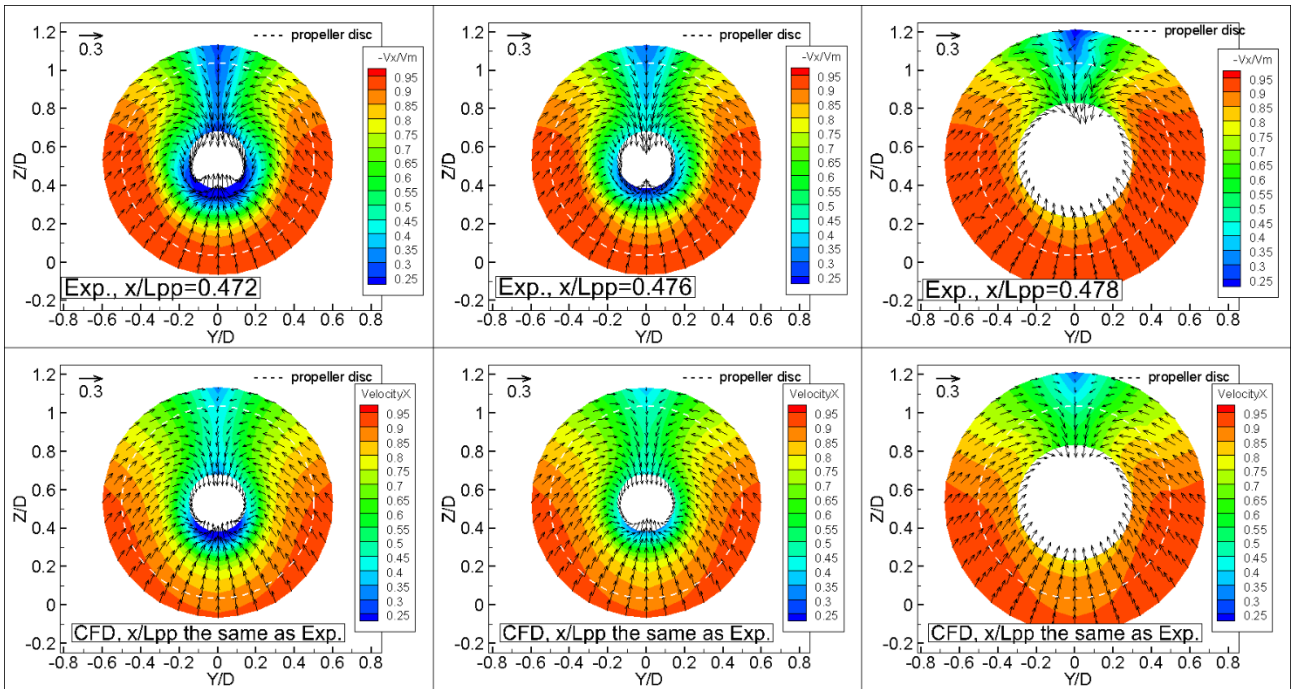

Figure 6: Experimental(top) and computational (bottom) results of total wake distribution at three different cross sections in model scale at x/L_{pp}=0.472 (left), 0.476 (middle) and 0.478 (right)

4.2 Full Scale

Figure 7 shows axial velocity profile from full scale computations evaluated at midship (x/L_{pp}, y/L_{pp})=(0.0, 0.0) vertically away from the ship bottom. In the result of smooth wall, 8 cells are located inside the viscous sub layer and transition region with y^+=1.4~1.6 which meets the minimum requirement (at least 3 points) suggested by ITTC[1]. For smooth wall result, simulated velocity profile follows wall-law very well. For rough wall result, the simulated velocity profile also agrees well to the reference line with ks=90(μm) suggested by Apsley (2007)[21], in the meantime, the log-law still holds. In the velocity profile shown in Fig. 7, the friction velocity u_τ for smooth wall and rough wall is approximately 0.026 and 0.029, respectively. It makes sense in that the computation with wall roughness gives larger wall shear stress which results in lager u_τ compared to smooth wall. According to the definition of $u^+(=u/u_\tau)$, it is also reasonable that estimated velocity profile and the reference line by Apsley (2007)[21] lie under wall-law without roughness, in other words, the log-law profile with roughness vertically shifts downward from the profile without roughness. Such trend is also reported by Ohashi (2019)[22] who applies roughness model to solve flows around tanker hull form.

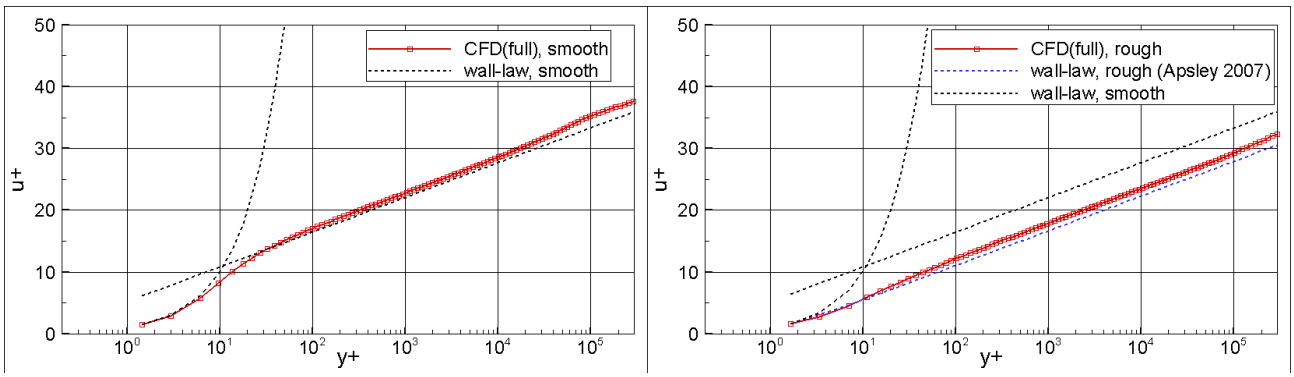

Figure 7: Axial velocity profile evaluated at midship (x/L_{pp}, y/L_{pp})=(0.0, 0.0) vertically away from the ship bottom: smooth wall (left) and rough wall (right)

Figures 8 and 9 show axial and tangential component of simulated nominal wake in full scale at x/L_{pp}=0.478. Axial component of simulated nominal wake in model scale shown in Fig. 5 is subjected to Sasajima-Tanaka extrapolation, and is added in Fig. 8. In Figs. 8 and 9, the parameter "θ=0°" corresponds to 12 o'clock position, and is positive toward clockwise direction observing from stern. The computational results indicate that the effect of current wall roughness become apparent up to r/R=0.5 to 0.6 for the present ship in both axial and tangential component. These results indicate that attention should be paid to the consideration of wall roughness when simulated nominal wake in full scale is utilized in designing propeller and ESDs.

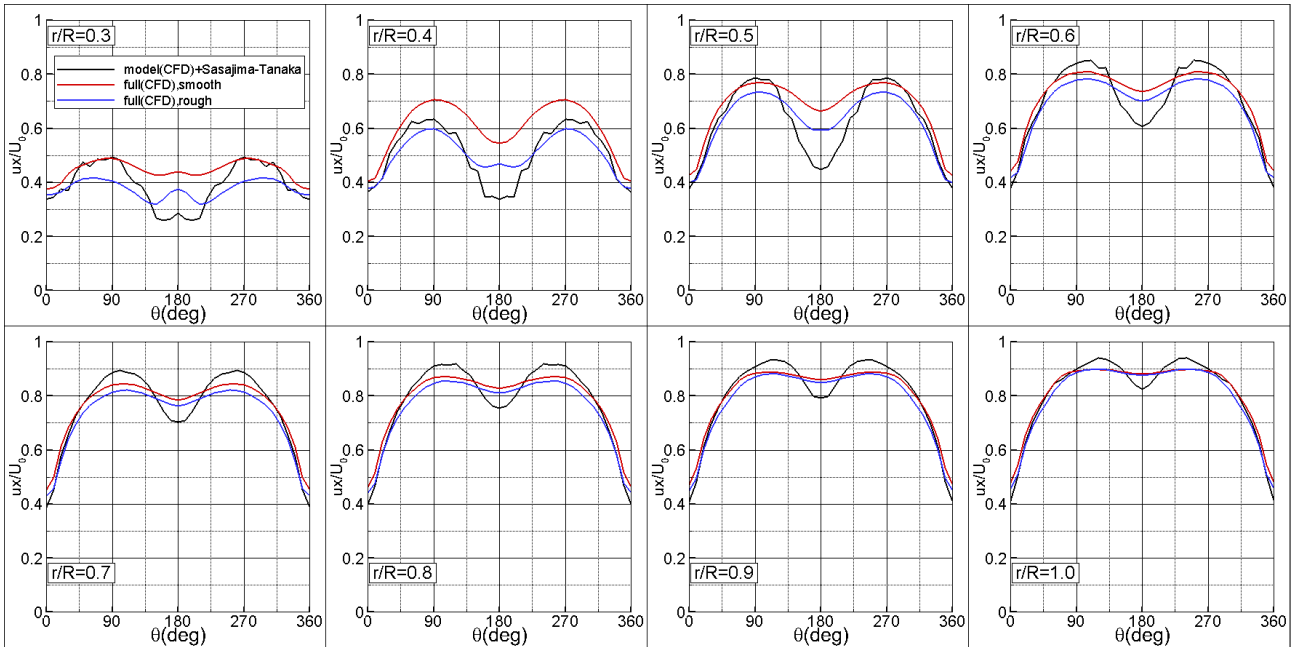

Figure 8: Simulated axial component of nominal wake in full scale at x/L_{pp}=0.478

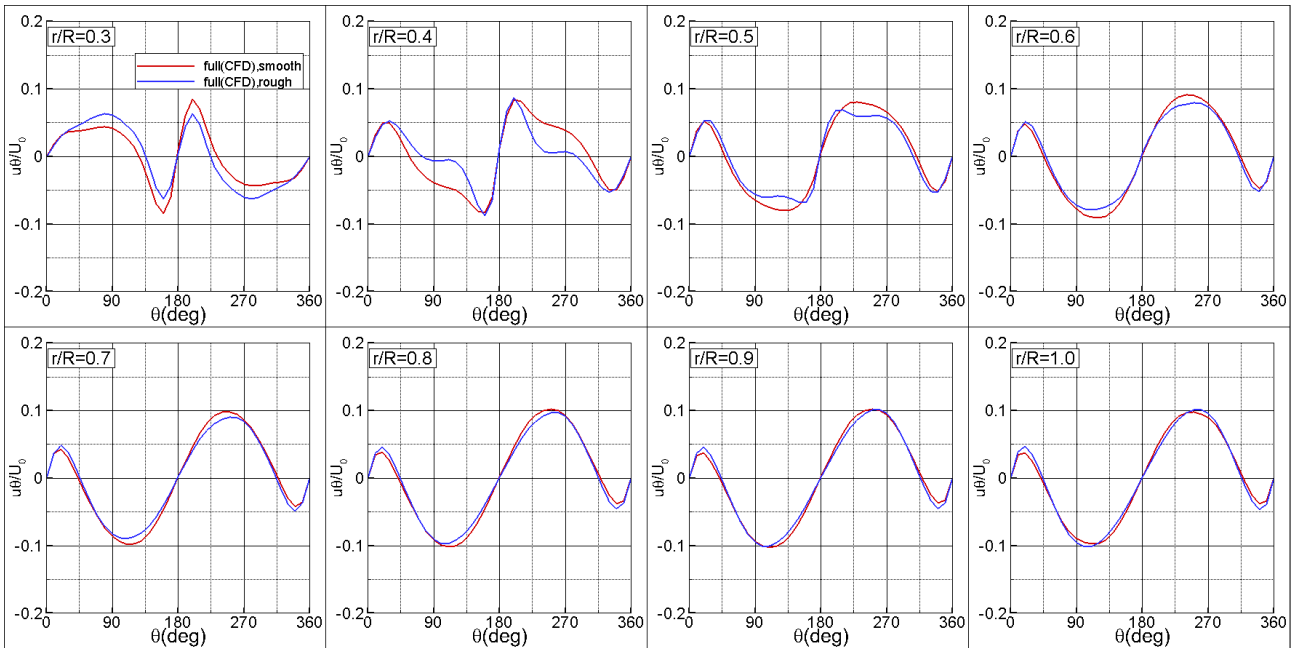

Figure 9: Simulated tangential component of nominal wake in full scale at x/L_{pp}=0.478

Table 4 compares e_i estimated from full scale CFD simulation and model scale CFD simulation with Yazaki's chart. The e_i estimated by CFD with rough wall is 3% smaller than that of estimated by CFD with smooth wall. The boundary layer in the stern vicinity becomes thicker due to wall roughness compared to the one without wall roughness which results in smaller e_i. The e_i estimated by Yazaki's chart implicitly includes the effect of wall roughness since the chart is based on full scale sea trial data, yet the present computational result without roughness gives closer value to the one from "Model CFD+Yazaki" than that from the result with roughness.

Table 4: Comparison of wake ratio e_i

Method	**e_i**
Model CFD+Yazaki	1.116
Full scale CFD (smooth)	1.127
Full scale CFD (rough)	1.090

Figure 10 shows validation results of axial ship wake in full scale at x/L_{pp}=0.477. When the wall roughness is taken into consideration in CFD simulation, the computational result apparently shows better distribution of total wake inside and outside of the propeller circle than that of the result without wall roughness. There are local discrepancies in velocity distribution between measurement and computation at 12 o'clock region and in the boss vicinity which are also common in the nominal wake in model scale.

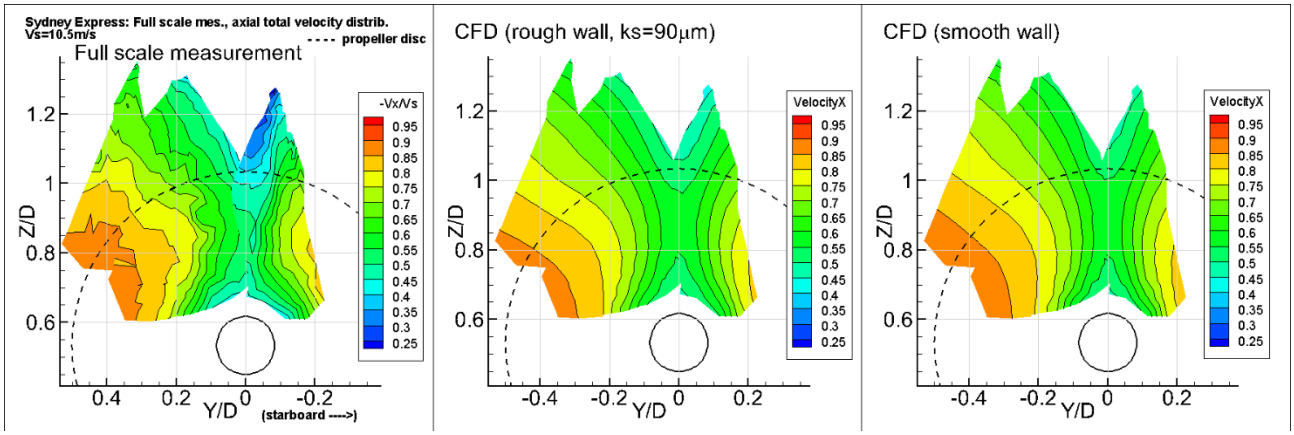

Figure 10: Validation of axial ship wake in full scale at x/L_{pp}=0.477: full scale measurement (left), computational result with smooth wall (middle), and computational result with rough wall (right)

Table 5 summarizes n_p, Q and P_D obtained from measurement and CFD, both in full scale, respectively. P_D is estimated as

$$P_D = 2\pi n_p Q \quad (1)$$

The np estimated by the present computation with wall roughness agree quite well with the measurement data within the difference of 0.5%, yet the computational results of Q and P_D show 6% to 10% of difference compared to the measurement data. The possible reason of these discrepancies may be due to 1) difference in roughness height between full scale measurement and CFD, 2) scale and roughness effects in POC and 3) difference in total wake shown in Fig. 10.

Table 5: Comparison of n_p(rps), Q(N-m) and P_D(MW)

Method	n_p (rps)	Q (N-m)	P_D(MW)
Full scale measurement	1.63	1.318E+06	13.5
Full scale CFD (smooth)	1.55	1.246E+06	12.1
Full scale CFD (rough)	1.61	1.500E+06	15.2

5 CONCLUSION

Viscous CFD simulations are carried out for conventional single-screw container ship "Sydney Express" in model and full scale using in-house finite volume RaNS solver NAGISA developed at NMRI. Structured grids are independently generated around hull and rudder, and domain connectivity information between the two blocks are calculated by in-house overset grid assembler UP_GRID also developed at NMRI. Rigorous validations are made both in model and full scale using available experimental data. In model scale, resistance and self propulsion coefficients are both well predicted by the present computation. Computational accuracy in nominal and total wake specifically at 12 o'clock and near the boss must be improved. In full scale, all the computational results and their validation against full scale measurement data indicate the importance of treatment of wall roughness.

ACKNOWLEDGEMENTS

The digitized data of measurement results in the wake field are provided by the courtesies of HSVA which is truly acknowledged.

REFERENCES

[1] ITTC Specialist Committee on CFD in Marine Hydrodynamics. "Practical guidelines for ship CFD applications". In: ITTC Recommended Procedures and Guidelines, 7.5-03-02-03 (2014).

[2] Tokyo 2015 A Workshop on CFD in Ship Hydrodynamics, http://www.t2015.nmri.go.jp/

[3] Hino et al. "Hull form design and flow measurements of a bulk carrier with an energy saving device for CFD validations". In: Proc. PRADS2016, Copenhagen, Denmark, 2016.

[4] ITTC Specialist Committee on Scaling of Wake Field. "Final report and recommendations to 26th ITTC". In: Proc. 26th ITTC Vol. II (2011), 379-417.

[5] Inukai et al. "Energy-saving principle of the IHIMU semicircular duct and its application to the flow field around full scale ships". IHI Engineering Review, 44, 1 (2011), 7-22.

[6] Sakamoto et al. "Viscous CFD analysis of stern duct installed on Panamax bulk carrier in model and full scale". In: Proc. 13th International Conference on Computer and IT Application in Maritime Industries, Redworth, UK, 2014.

[7] Sakamoro et al. "Evaluation of hydrodynamic performance of pre-swirl and post-swirl ESDs for merchant ships by numerical towing tank procedure". In: Ocean Engineering, 178 (2019), 104-133.

[8] Ponkratov D. Ed. Proc. 2016 Workshop on Ship Scale Hydrodynamic Computer Simulation, LR Reference Ref. 8428, 2017.

[9] Kleinwachter et al. “Full scale total wake field PIV measurements in comparison with ANSYS CFD calculations: a contribution to a better propeller design process”. In: Journal of Marine Science and Technology, 22, 2 (2017), 388-400.

[10] Joint Research Project (JoRes): Development of an industry recognized benchmark for ship energy efficiency solutions (https://jores.net/)

[11] Ohashi et al. “Development of a structured overset Navier-Stokes solver with a moving grid and full multigrid method”. In: Journal of Marine Science and Technology. https://doi.org/10.1007/s00773-018-0594-7. (2018).

[12] Hellsten A. “Some improvements in Menter’s k-ω SST turbulence model”. AIAA paper-98-2554 (1997).

[13] Kobayashi H. and Kodama Y. “Developing spline based overset grid assembling approach and application to unsteady flow around a moving body”. In: Journal of Mathematics and System Science, 6 (2016), 339-347.

[14] Keller A.P. and Weitendorf E.A. “A determination of the free air content and velocity in front of the “Sydney-Express” propeller in connection with pressure fluctuation measurements”. In: Proc. 12th Symposium on Naval Hydrodynamics, 1979, 301-323.

[15] Kux et al. “LDV-Nachstrommessungen auf der “Sydney Express””. Technische Universitat Hamburg-Harburg, 1982.

[16] 18th ITTC Cavitation Committee. “Report of cavitation committee”. In: Proc. 18th ITTC, 1(1988), 159-219.

[17] Ukon Y. “Study on experimental prediction on ship hull vibration induced by propeller and cavitation”. In: Technical Bulletin of Ship Research Institute. 4(1991), 193-226.

[18] Orito H. and Kakinuma M. “On the relationship between surface roughness of a ship and reduction in ship speed”. In: Bulletin of the Society of Naval Architects of Japan. 616 (1980), 540-545.

[19] Schweighofer et al. “Viscous-flow computations of two existing vessels at model- and full-scale ship Reynolds number – a study carried out within the European Union project, EFFORT.” In: Proc. International Conference on Computational Methods in Marine Engineering (MARINE), 2005.

[20] Sakamoto et al. “Computational study for single-screw and twin-skeg container ships in full scale by unstructured grid based RANS solver”. In: Proc. JASNAOE Annual Fall Meeting. 13 (3011), 221-224.

[21] Apsley D. “CFD calculation of turbulent flow with arbitrary wall roughness”. In: Flow Turbulence Combust. 78 (2007), 153-175.

[22] Ohashi K. “Numerical study of roughness model effect at actual ship scale”. In: Proc. International Conference on Computational Methods in Marine Engineering (MARINE), 2019, 694-705.